PERGAMON

Journal of Structural Geology 25 (2003) 421–440

JOURNAL OF STRUCTURAL GEOLOGY

www.elsevier.com/locate/jsg

Late Cretaceous–early Tertiary Laramide deformation of the northern Colorado Plateau, Utah and Colorado

Alexander P. Bump*, George H. Davis

Department of Geosciences, The University of Arizona, Tucson, AZ 85721, USA

Received 13 December 2000; received in revised form 28 November 2001; accepted 26 February 2002

Abstract

The structure of the northern Colorado Plateau is dominated by a series of highly asymmetrical, presumably fault-cored anticlines: the Kaibab, Circle Cliffs, Miners Mountain, San Rafael Swell, Monument, and Uncompahgre uplifts. In map view, they are irregularly distributed with widely varying sizes and orientations. In Permian through Jurassic rocks, interpretations of outcrop-scale structures, including jointed Eshelby inclusions, stylolites, en échelon vein arrays, deformation bands and meso-scale faults, show principal stress directions that are consistently oriented within each uplift, but vary considerably between uplifts. In general, the results indicate that there are two groups of uplifts, one of which shows evidence of NE–SW-directed compressive stress, and another which shows evidence of NW–SE-contraction. Because deformation in the sedimentary cover is forced by differential movement of basement fault blocks, cover stress patterns may be interpreted as basement strain patterns. These results are similar to the kinematic interpretations of Kelley and Clinton (1960) and highlight the importance of oblique slip. Finally, examination of structural contours allows the interpretation of basement strain magnitudes and indicates that the major faults are not interconnected.

Keywords: Laramide; Monoclines; Colorado Plateau; Structure; Kinematics

1. Introduction

Since their first descriptions by Powell (1873) and Dutton (1882), the enigmatic monoclines of the Colorado Plateau have been the subject of structural inquiry. There are 10 major monoclines on the Plateau, each forming one side of a highly asymmetrical anticline or 'uplift'. In map view, the uplifts show irregular orientation and distribution, precluding easy kinematic interpretation. Some trend northeasterly and others southeasterly. Moreover, several of the bounding monoclines display markedly curved traces. At depth, the uplifts are interpreted to pass into faulted basement (Figs. 1 and 2; Kelley, 1955; Davis, 1978; Stern, 1992; Tindall and Davis, 1999). The interpretation is based on a number of factors: (1) the uplifts correspond to gravity highs (Cook et al., 1991; Stern, 1992); (2) in the cases of the Kaibab and Uncompahgre uplifts, the basement is visible at the surface (Lohman, 1965; Cashion, 1973; Huntoon and Sears, 1975; Stone, 1977; Huntoon, 1993); (3) COCORP seismic data show a basement high beneath the San Rafael Swell (Allmendinger et al., 1987); and (4) the uplifts are superficially similar to other, better studied uplifts in Wyoming and Colorado that are known to be basement-cored. Where exposed, these basement faults are ancient features that show multiple episodes of slip, further complicating the kinematic picture (e.g. Huntoon and Sears, 1975; Stone, 1977; Huntoon, 1993).

Driven at various times by oil exploration, the search for uranium, and pure curiosity, much classic geologic work has been done on Colorado Plateau uplifts (Powell, 1873; Gilbert, 1876; Dutton, 1882; Gilluly, 1929; Baker, 1935; Strahler, 1948; Eardley, 1949; Kelley, 1955; Kelley and Clinton, 1960). In many ways these uplifts are similar to those of the Rocky Mountains in Wyoming and Colorado. All are contractional, low temperature, basement-cored structures controlled by reverse faults, which appear to cut much or all of the crust. All show similarly irregular orientation and distribution and all are products of the Late Cretaceous–early Tertiary Laramide orogeny (Huntoon and Sears, 1975; Davis, 1978; Brown, 1993; Erslev, 1993). Much more is known about the structure and kinematics of Rocky Mountain uplifts, however. Extensive seismic and borehole data have defined much of the shallow subsurface structure; and exposure of the major basement faults (e.g. Lowell, 1983; Schmidt et al., 1993) and associated minor faults has permitted effective paleostress analysis and kinematic interpretation (e.g. Molzer and Erslev, 1992; Erslev, 2001).

* Corresponding author.
E-mail address: abump@geo.arizona.edu (A.P. Bump).

0191-8141/03/$ - see front matter © 2002 Elsevier Science Ltd. All rights reserved.
PII: S0191-8141(02)00033-0

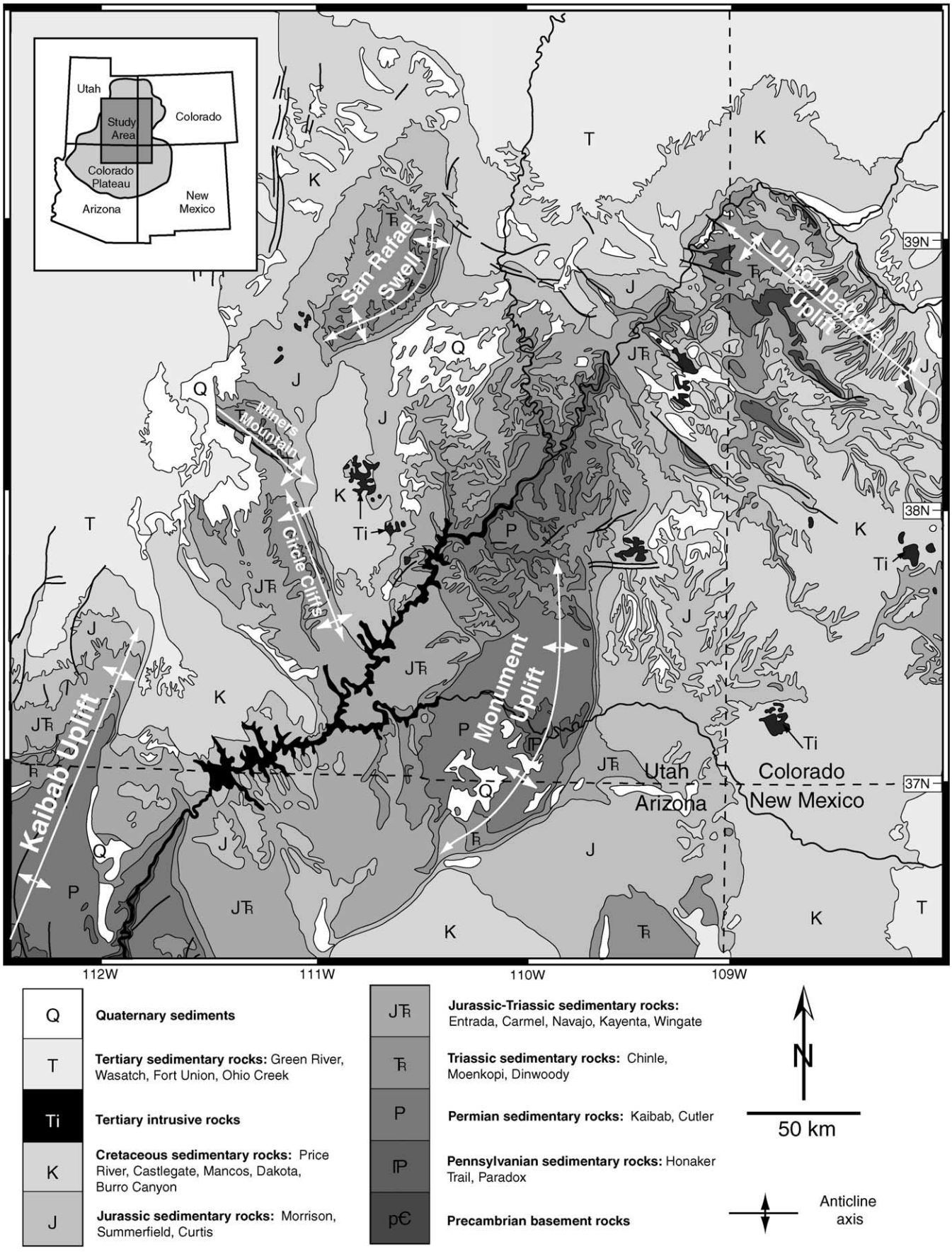
Utah
Study Area
Colorado
Colorado Plateau
Arizona
New Mexico
San Rafael Swell
Uncompahgre Uplift
Monument Uplift
Kaibab Uplift
Circle Cliffs
Miners Mountain
39N
38N
37N
112W
111W
110W
109W
Utah
Colorado
Arizona
New Mexico
Q Quaternary sediments
T Tertiary sedimentary rocks: Green River, Wasatch, Fort Union, Ohio Creek
Ti Tertiary intrusive rocks
K Cretaceous sedimentary rocks: Price River, Castlegate, Mancos, Dakota, Burro Canyon
J Jurassic sedimentary rocks: Morrison, Summerfield, Curtis
JTr Jurassic-Triassic sedimentary rocks: Entrada, Carmel, Navajo, Kayenta, Wingate
Tr Triassic sedimentary rocks: Chinle, Moenkopi, Dinwoody
P Permian sedimentary rocks: Kaibab, Cutler
PP Pennsylvanian sedimentary rocks: Honaker Trail, Paradox
pC Precambrian basement rocks
N
50 km
Anticline axis

Fig. 2. San Rafael monocline, near Eardley Canyon. View is toward the north. The prominent flatirons in the center-right of the photo are Jurassic Navajo and Wingate Sandstone. The dipslope along the horizon line to the left is Permian Kaibab Limestone.

In the Colorado Plateau, sedimentary cover is retained over the crests of the uplifts, obscuring the basement faults but also preserving a record of uplift-induced stress that is not present elsewhere in the Laramide province. A number of studies have tried to take advantage of this, mapping joint patterns in an effort to interpret the kinematics of the uplift formation (e.g. Kelley and Clinton, 1960; Bergerat et al., 1992). These attempts have largely been inconclusive, due to the complexity of the joint patterns and the difficulty in interpreting the origin(s) of the joints. Recent recognition of other classes of penetrative structures in the Colorado Plateau, however, offers a new opportunity for interpretation of paleostress directions. The purpose of this paper is: (1) to describe these small-scale structures and their paleostress significance, (2) to present paleostress analysis of the Miners Mountain, San Rafael, Monument and Uncompahgre uplifts, and (3) to combine the results with other recent work to create a map of basement strain patterns for the northern Colorado Plateau.

2. Methodology

2.1. General considerations

The approach used in this study relies on mapping the small-scale, penetrative structures that are present only within and near the steep limb of each uplift. The spatial association of the structures described here with the monoclines strongly suggests that the two are genetically related, that the penetrative structures are either subsidiary products of monoclinal folding or that they are products of the same stresses that formed the monoclines. In order to separate local strains related to folding from those reflecting shortening directly related to formation of the uplift, we have taken advantage wherever possible of map-view curves in the monoclines. For each monocline, field areas for detailed study were chosen to span the widest possible range of trend for that monocline (see for example the San Rafael Swell, Fig. 1). If the structures mapped were subsidiary consequences of monoclinal folding (e.g. crowding within the synclinal hinge), then it is expected that they would everywhere maintain a constant orientation relative to the monocline. For example, in the case of contractional structures related to crowding within the synclinal hinge, it is expected that contraction would everywhere be perpendicular to the axial trend of the monocline, no matter how that trend might vary. On the other hand, if the structures mapped are reflective of the shortening direction for the uplift as a whole, it is expected that they will maintain a constant orientation, regardless of the trend of the associated monocline. The further possibilities that cover and basement are detached or that strain is partitioned (e.g. Varga, 1993) are discounted because of the observation that the methodology employed here is capable of revealing oblique slip where present (Tindall and Davis, 1999).

It is also important to demonstrate that the strains documented here are contemporaneous with the Laramide deformation of the Colorado Plateau since at least two of the uplifts have multiple episodes of slip on their bounding faults. The Uncompahgre uplift for example was active in the Pennsylvanian Ancestral Rockies event (Stone, 1977) and the fault coring of the East Kaibab monocline has at least four episodes of slip, shown by different offsets at different stratigraphic horizons (Huntoon and Sears, 1975; Huntoon, 1993). In almost all cases, the structures described here are hosted in Jurassic and younger rocks, ruling out the possibility that they are the result of Pennsylvanian Ancestral Rockies tectonism. Where structures are hosted in older rocks, they are kinematically compatible with similar structures in adjacent Jurassic rocks, implying that all of the deformation is Jurassic or younger. Limited thermochronology (Dumitru et al., 1994) and sedimentologic study (Lawton, 1983a,b; Goldstrand, 1994), as well as regional timing considerations (Brown, 1988; Dickinson et al., 1988) lead to the conclusion that the Colorado Plateau uplifts formed in the latest Cretaceous to early Tertiary ($\sim$72– $\sim$ 55 Ma). Thus the possibility also exists that some of the deformation reported here may be the product of mid-Tertiary igneous intrusion and reactivation of earlier structures (Jackson and Pollard, 1990; Davis, 1999). We feel that any such reactivation must have been minor in comparison with the main period of deformation (Laramide), which was sufficient to produce the aforementioned thermochronolgic and sedimentologic record and we note that the datasets that we present show a coherent picture with little scatter.

2.2. Useful structures

This study relies on a number of penetrative structures

Fig. 1. Geologic map (after Bennison, 1990) of the northern Colorado Plateau and generalized stratigraphic column showing common formations.

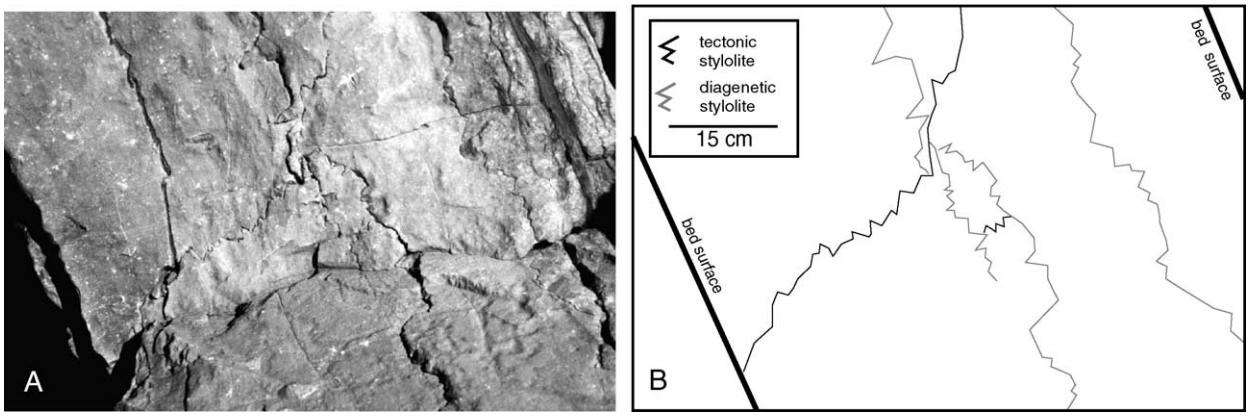

Fig. 3. Stylolites. (A) Photograph of a stylolite-bearing limestone bed within the Jurassic Carmel Formation on the San Rafael Swell. (B) Tracing of photo highlighting diagenetic stylolites (teeth perpendicular to bedding) and tectonic stylolites (teeth parallel to bedding).

whose kinematic significance has not yet been fully exploited in the Colorado Plateau. These include stylolites, en échelon vein arrays, Eshelby joints, deformation bands, and meso-scale faults. This approach is designed to maximize the information to be gleaned from available exposures and relies on previous studies which have shown that analysis of small structures can yield reliable paleostress histories (e.g. Nickelsen, 1979; Eyal and Reches, 1983; Hancock, 1985; Gray and Mitra, 1993). The exact suite of structures present in a given area is dependent on the local lithology and magnitude of strain and rarely includes all of the structures described here. These relationships are described below.

2.2.1. Stylolites

Stylolites occur in many rock types but are particularly common in marly limestones (e.g. Davis and Reynolds, 1996). They may be described as serrated surfaces with interlocking teeth, typically enclosing a thin clay seam (Fig. 3; Nickelsen, 1972). Spacing between stylolites is generally on the order of several centimeters to a few meters (e.g. Davis and Reynolds, 1996). In the northern Colorado Plateau region, they are most commonly found in limestones of the Jurassic Carmel Formation and the Pennsylvanian Honaker Trail Formation. Within those units, they may be present at very low strains, that is at bedding dips as low as 10°.

Stylolites are interpreted to be the product of pressure solution and to represent a maximum compressional stress (σ_1) parallel to the long axis of their teeth. Two types are commonly recognized. Those with teeth perpendicular to bedding are thought to reflect lithostatic loading and were not considered in this study. Those with teeth parallel to bedding are thought to reflect non-hydrostatic tectonic shortening (e.g. Twiss and Moores, 1992; Dunne and Hancock, 1994; Davis and Reynolds, 1996) and are discussed below.

2.2.2. Eshelby joints

Eshelby joints are defined as parallel or subparallel joints hosted within mechanically stiff inclusions that in turn are surrounded by a compliant matrix (Eidelman and Reches, 1992). The joints do not extend into the matrix (Fig. 4). In the area of this study, such joints are found within chert nodules in the Permian Kaibab Limestone and Pennsylvanian Honaker Trail Formation. The nodules are sub-circular and range in size from 3 to 25 cm in diameter. Joints within the nodules are typically spaced approximately 1 cm apart. Often there are two sets, one relatively straight and continuous, the other more curviplanar and abutting joints of the first set, at approximately right angles.

Eshelby joints are interpreted to form from tensile failure due to the amplification of tectonic stresses within mechanically stiff inclusions (Eshelby, 1957; Eidelman and Reches, 1992). The minimum compressional stress (σ_3) direction is perpendicular to the joint surface. The σ_1 axis thus lies within the plane of the joint and given the tectonic origin of the joint, is assumed to be horizontal, parallel to the average strike of the dominant (i.e. straight and continuous) joint set. Eshelby joints have been shown to be reliable tectonic paleostress indicators (e.g. Eidelman and Reches, 1992).

2.2.3. En échelon arrays of semi-brittle structures

En échelon arrays consist here of short stylolites and calcite veins oriented at approximately right angles to each other and distributed along a linear zone in a stepping or en échelon fashion (Fig. 5; Shainin, 1950; Hancock, 1972; Ramsay and Huber, 1987). Though they are common in sandstone, dolostone, and limestone, their occurrence within the study area is limited to limestones of the Pennsylvanian Honaker Trail Formation where they are commonly on the order of a few meters in length and a few centimeters in width.

En échelon arrays are interpreted to represent semi-brittle shear zones, the sense of shear on which is given by the intersection geometry between individual veins and the axis of the array (Fig. 5). Progressive shear rotates early-formed veins and stylolites, which are eventually

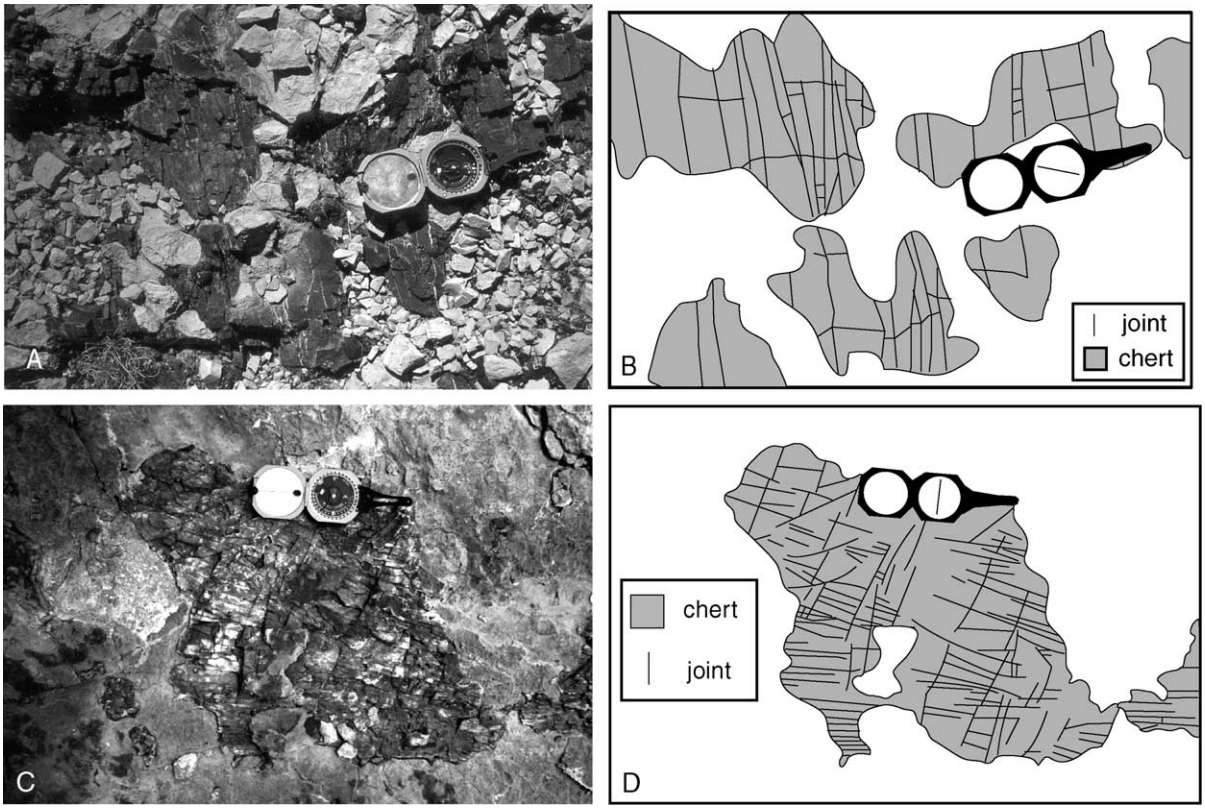

Fig. 4. Eshelby joints. (A) and (B) Photo and tracing of jointed chert nodules in limestone of the Pennsylvanian Honaker Trail on the Monument uplift. Note that joints do not extend into limestone. Brunton compass for scale. (C) and (D) Photo and tracing of jointed chert nodules in limestone of the Pennsylvanian Honaker Trail on the Monument uplift. Note that joints do not extend into limestone. Brunton compass for scale.

replaced by new, more favorably oriented ones (Ramsay and Huber, 1987). Because of this and the debate over whether such arrays represent stress or strain (Dunne and Hancock, 1994), interpretation of the strain significance of individual arrays is fraught with difficulty. In the case of conjugate en échelon arrays, however, the interpretation is quite straightforward: the σ_1 direction bisects the acute angle between the conjugate arrays and is perpendicular to the intersection line of the conjugates (Shainin, 1950; Hancock, 1972; Ramsay and Huber, 1987; Craddock and van der Pluijm, 1988; Dunne and Hancock, 1994).

2.2.4. Deformation bands

Deformation bands are small faults characteristic of porous sandstones. They are characterized by a narrow zone of cataclasis and collapse of pore space of the host sandstone (Aydin, 1978; Aydin and Johnson, 1983). Individual bands typically exhibit displacements of a few millimeters or less. Larger displacements are accomplished by the formation of new bands adjacent to the first. In places, this results in thick zones of aggregated deformation bands, with up to several meters of offset. In the northern Colorado Plateau, zones of deformation bands commonly exhibit a conjugate Riedel geometry (Cloos, 1928; Riedel, 1929) with en échelon R surfaces connected by R′ surfaces (Fig. 6; Davis et al., 2000. Additionally, slickenlines are sometimes present. Within the study region, deformation bands are found primarily in the Jurassic Entrada, Navajo and Wingate formations, the most porous of the exposed sandstones in the region. Both dip-slip and strike-slip deformation bands are abundant, albeit at differing study areas.

The interpretation of strain significance is based on work by Tchalenko (1970), Wilcox et al. (1973), and Davis et al. (2000). The sense of slip on individual deformation band zones is interpreted on the basis of Riedel geometries and offset markers. In the absence of slickenlines, slip direction is interpreted to lie within the plane of the deformation band array and to be perpendicular to the line of intersection between R and R′ surfaces. In the case of conjugate strike-slip bands, the σ_1 direction is taken as the acute bisector between right- and left-handed arrays. For reverse-slip bands, the map-view projections of the σ_1 direction is interpreted as parallel to the trend of the slip direction (Davis and Reynolds, 1996).

2.2.5. Meso-scale faults

Meso-scale faults are defined here as brittle faults ranging in scale from outcrop to a few tens of meters in length. Slip magnitudes are typically on the order of

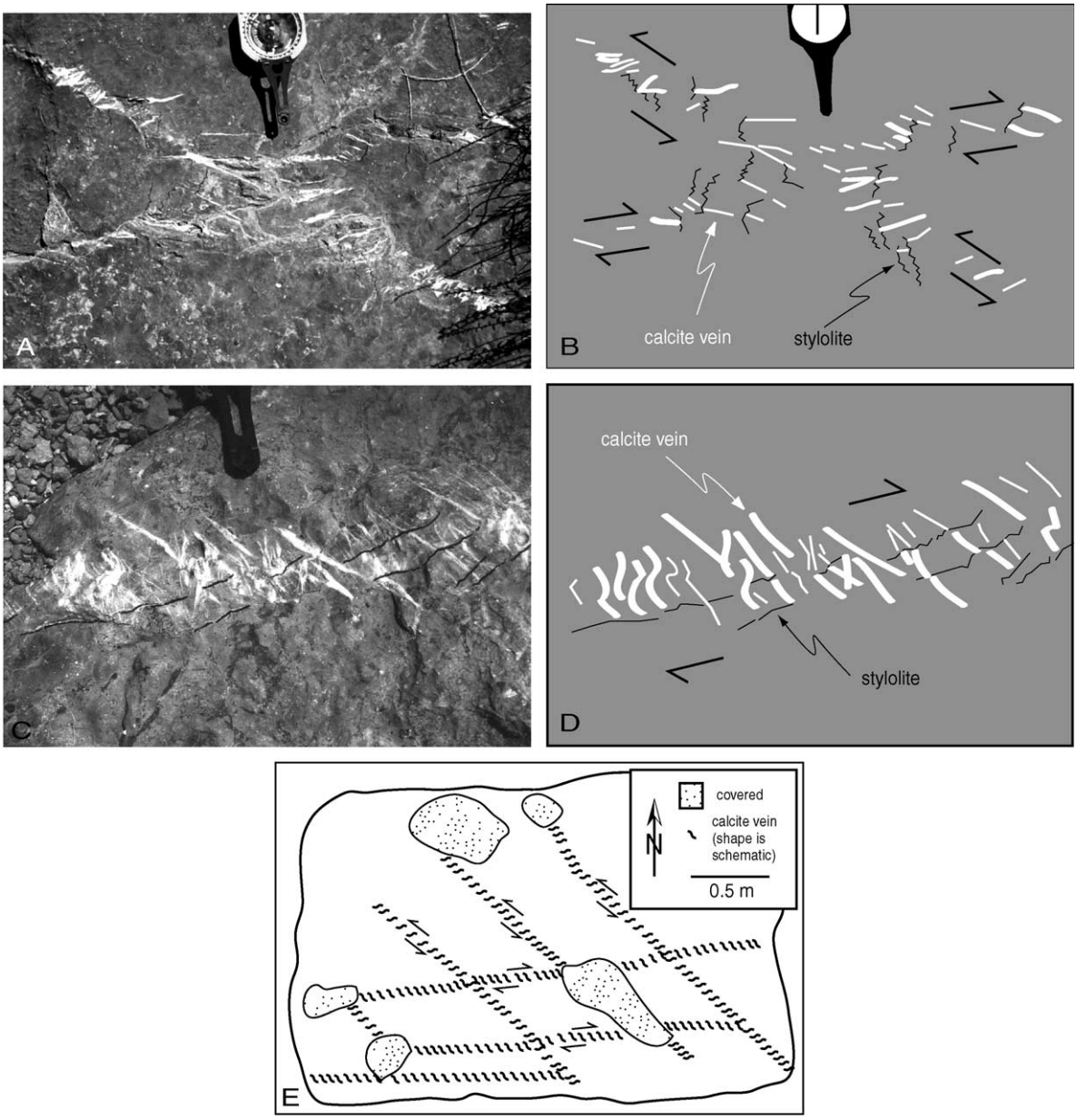

Fig. 5. (A) and (B) Photo and tracing of conjugate en échelon arrays of veins and stylolites in limestone of the Pennsylvanian Honaker Trail Formation. Arrows show sense of shear. Brunton compass for scale. (C) and (D) Photo and tracing of a detail of a similar array, also in the Honaker Trail Formation. Stylolites in the photo are traced in black to enhance visibility. Note that there are multiple generations of veins present, showing varying degrees of rotation. Tip of a Brunton compass for scale. (E) Tape and compass map of en échelon vein arrays in one particularly well-exposed outcrop on the Monument Uplift.

centimeters to a few meters. Well-developed slickenlines were often present. Faults were not restricted to any particular lithology.

For this study, interpretation of the strain significance of faults is similar to that employed for deformation bands. Conjugate strike-slip faults were interpreted by separately plotting left- and right-handed faults and their associated slickenlines on a stereonet. The σ_1 direction was interpreted as the acute bisector between left- and right-handed faults. For dip-slip faults, the map-view projection of the σ_1 direction was interpreted as parallel to the slip lineations (Davis and Reynolds, 1996).

3. Field analysis

3.1. San Rafael Swell

The San Rafael Swell is a highly asymmetric, doubly plunging anticline located in central Utah on the northwestern edge of the Colorado Plateau (Fig. 7). It is approximately 130 km long by 55 km wide with a NNE-trending axis (Kelley, 1955). The western limb of the uplift is a broad, gentle homocline while the east limb is the steep San Rafael monocline. In map view, the monocline is convex to the southeast (Hintze, 1980). At its northern

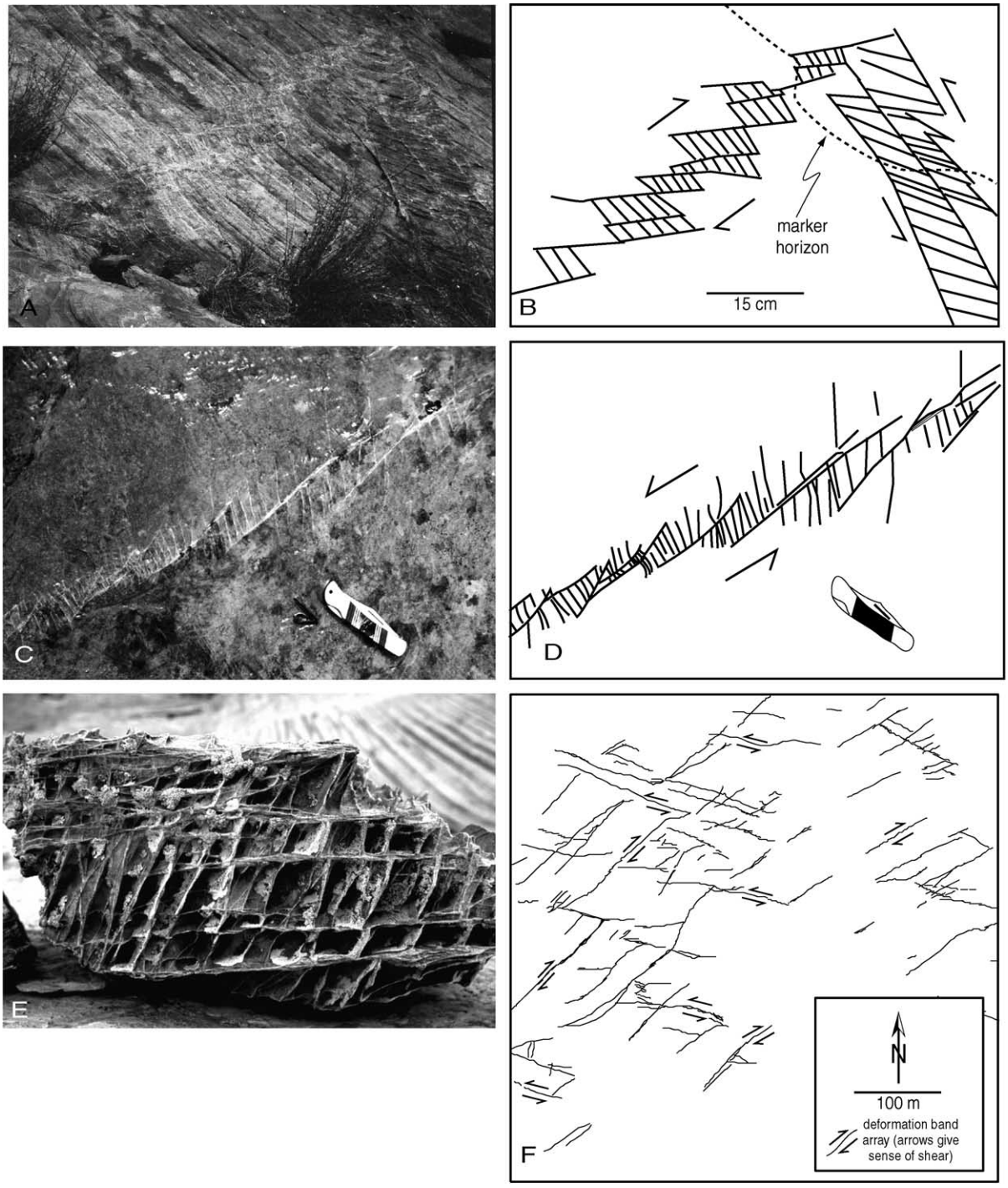

Fig. 6. (A) and (B) Photo and tracing of conjugate reverse-slip deformation bands offsetting cross beds of Jurassic Navajo Sandstone. Note Riedel geometry in deformation bands. Photo was taken in Cairn Canyon on the San Rafael Swell. (C) and (D) Photo and tracing of strike-slip deformation band ladders in Jurassic Navajo Sandstone on Miners Mountain. Shear is left-lateral. Pocket knife for scale. (E) Float block of Jurassic Navajo Sandstone on Miners Mountain. Undeformed sandstone has weathered out, leaving the more resistant deformation band ladders. R segments are horizontal in photo and R′ segements are sub-vertical. Sense of shear is top to the left. Block is approximately 1 m wide. (F) Portion of a structure map of the Sheets Gulch study area on Miners Mountain showing deformation arrays (after Davis, 1999; Davis et al., 2000). Digital cartography by GEO-MAP, Inc., Tucson, Arizona.

extreme it strikes approximately N–S with a maximum limb dip of less than 20°E. Southward, bedding steepens toward a maximum dip of about 70° a few kilometers south of I-70, then shallows back to 25° as the monocline curves westward. Continuing to curve toward a strike of N70°E at its southern end, the middle limb of the monocline steepens again to a dip of 40°. The maximum structural relief on the uplift is approximately 1.3 km (Kelley, 1955).

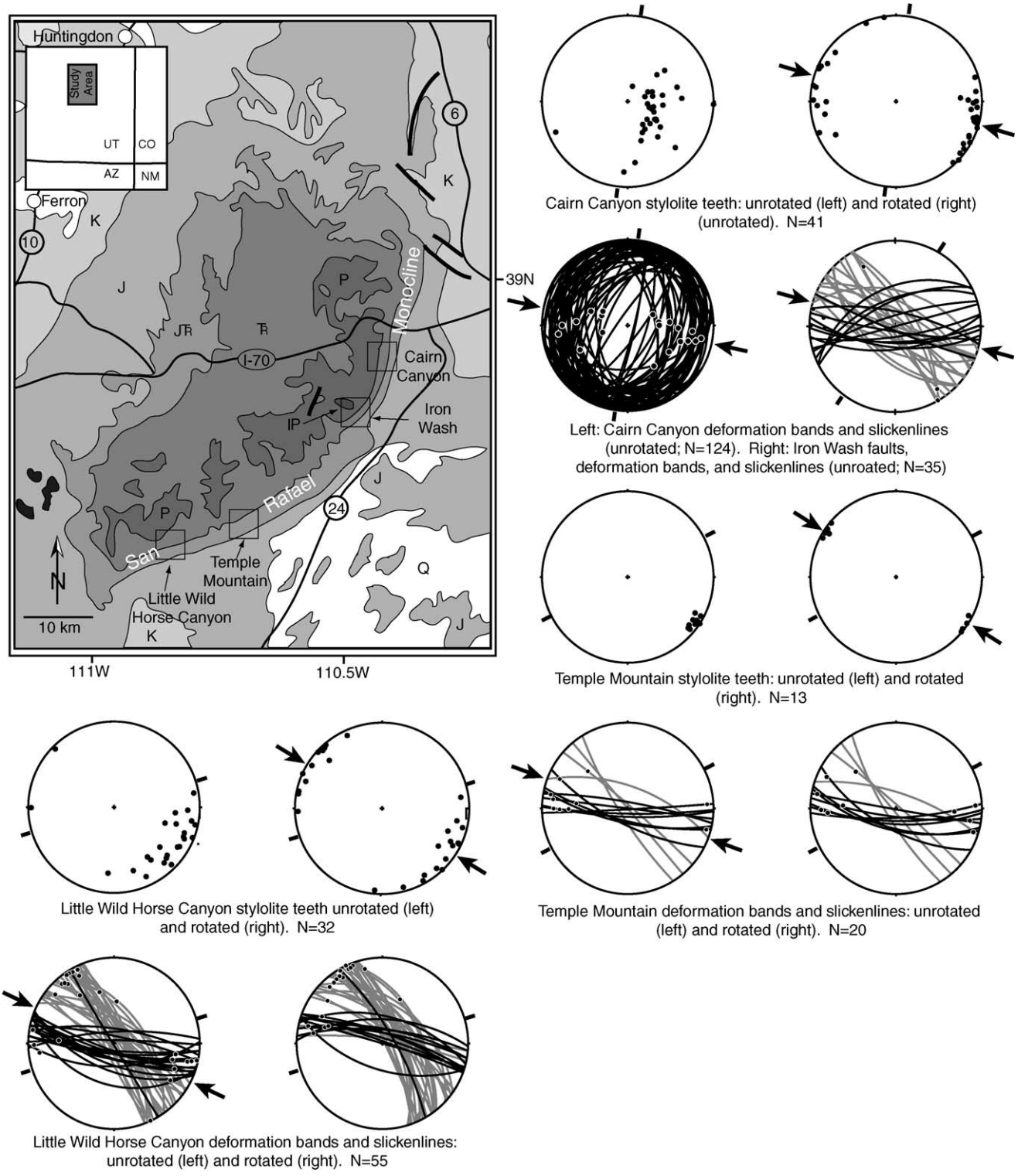

Fig. 7. Geologic map of the San Rafael Swell region (after Bennison, 1990) and lower hemisphere equal area stereoplots showing orientations of deformation bands, slickenlines and stylolite teeth. With the exception of deformation bands at Cairn Canyon and Iron Wash, orientations are shown both as measured ('unrotated') and rotated such that bedding is returned to horizontal ('rotated'). Strike-slip deformation bands (Iron Wash, Temple Mountain and Little Wild Horse Canyon) are shaded according to slip sense: left-handed deformation bands are shown in gray, right-handed ones in black. The Cairn Canyon area contains only reverse-slip deformation bands which are all shown in black. Paired arrows on each plot show the interpreted σ_1 direction based on the information within that plot. Paired heavy black tick marks on the outside of each plot show the local strike of the basement fault (which is assumed to parallel the strike of the monocline). Location map shows the area portrayed in Fig. 1.

The penetrative structures examined in this study are most abundant where bedding dip is steeper than about 30°. Fieldwork thus focused on four areas within the steeper sections of the fold (Fig. 7). Cairn Canyon is located just south of I-70 in an area where maximum bedding dip is about 65°. Iron Wash is situated several kilometers south of Cairn Canyon at a prominent kink in the trend of the monocline. This location also coincides with an abrupt change in maximum bedding dip from about 65° on the north side to about 30° on the south side. Temple Mountain is located a few kilometers south of that, with a steepest bedding orientation of 30°. Finally, Little Wild Horse Canyon is near the southern end of the monocline, where bedding strikes approximately N50°E and reaches a maximum dip of 45°. The map areas thus span a range of 50° in the strike of the monocline. Each of the areas is approximately 5 km square, is centered on exposures of the Jurassic Navajo Sandstone and includes rocks as old as the Permian Cutler Group and as young as the Jurassic Morrison Formation. Mapping was carried out on foot, in both canyons and, where possible, on the ridges between canyons. Two types of structures were mapped: stylolites and deformation bands.

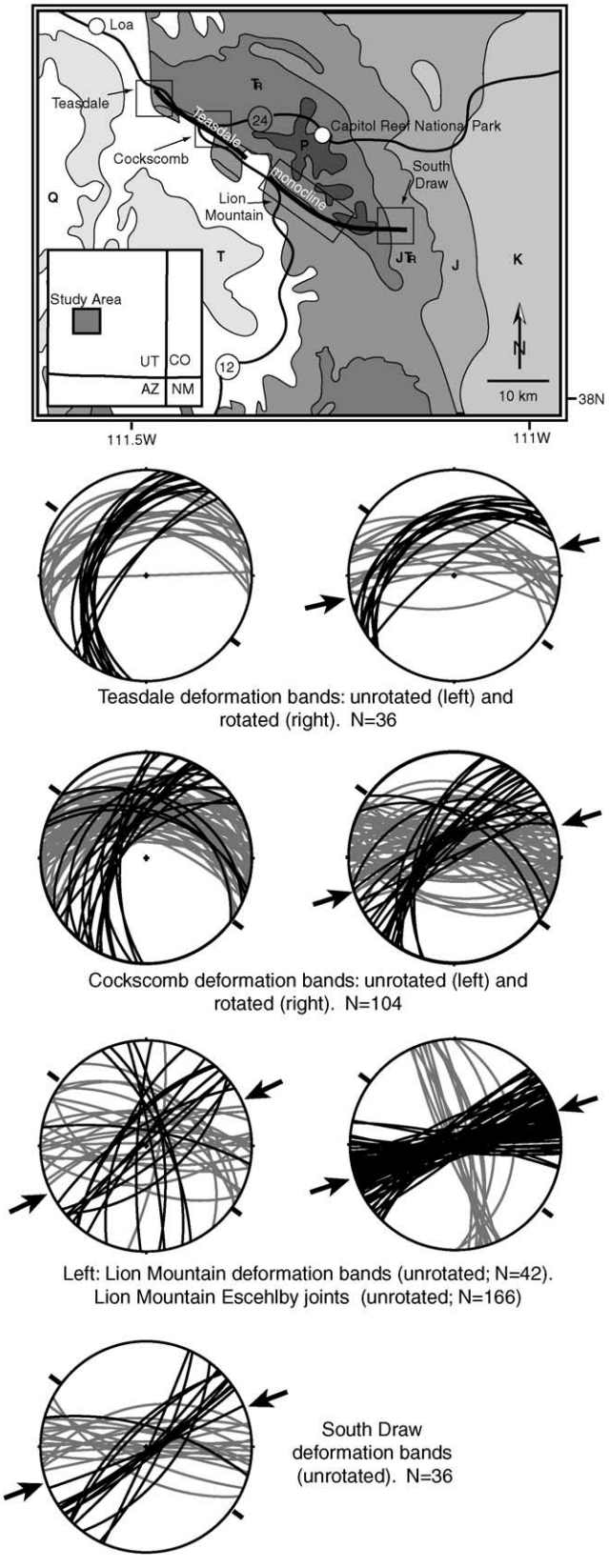

3.1.1. Stylolites

Tectonic stylolites (i.e. ones with teeth not perpendicular to bedding) on the San Rafael Swell were found exclusively within a single limestone bed near the base of the Jurassic Carmel Formation. The teeth are approximately parallel to bedding regardless of the current bedding attitude. When rotated such that bedding is returned to horizontal, the trend of the teeth is approximately S55°E (Fig. 7).

The consistency of orientation and the spatial association of stylolites with the monocline are interpreted as evidence that the trend of the teeth records the σ_1 direction for the San Rafael Swell: ~S55°E. That bedding must be returned to horizontal in order for the stylolite orientations to cluster is interpreted as evidence that pressure solution was active primarily in the early phases of folding.

3.1.2. Deformation bands

Deformation bands are found only within the porous sandstones and are most abundant in the Jurassic Navajo and Wingate Sandstones but are also present within the Jurassic Entrada Formation and in the sandstones of the Permian Cutler Group. At Cairn Canyon, where the monocline trends about N10°E, deformation bands are almost

Fig. 8. Map of the Miners Mountain region (after Bennison, 1990) and lower hemisphere equal area stereonets of deformation band and Eshelby joint orientations. All deformation bands are strike-slip and are shaded according to slip sense: left-handed deformation bands are shown in gray, right-handed ones in black. Orientations for deformation bands at the Teasdale and Cockscomb sites are shown both as measured ('unrotated') and rotated such that bedding is returned to horizontal ('rotated'). Orientations at the other locations have not been rotated as bedding is both poorly defined and close to horizontal already. The Eshelby joint plot shows primary joints in black and secondary ones in gray. Paired arrows on each plot show the interpreted σ_1 direction based on the information within that plot. Paired heavy black tick marks on the outside of each plot show the local strike of the basement fault (which is assumed to parallel the strike of the monocline). Location map shows the area portrayed in Fig. 1.

exclusively reverse-slip and exhibit multiple, cross-cutting generations, dipping both east and west (Fig. 7). Each generation appears to have formed, been rotated along with the steepening beds, and subsequently been cross-cut by a new, more favorably-oriented generation. At the other three field areas, where the monocline swings to a more easterly trend, deformation bands are primarily strike-slip. Both right- and left-handed zones are present, and mutually cross-cut, indicating that they are a conjugate pair. The right handed zones are generally much better developed however, reaching as much as 50 cm in thickness. Left-handed zones of deformation bands are generally less frequent and rarely exceed a few centimeters in width, suggesting that they have accommodated far less slip. In none of the field areas do the deformation band orientations cluster noticeably better when bedding is returned to horizontal than they do as they were measured in the field.

Because they reflect essentially dip-slip, the stress significance of the reverse-slip deformation bands is readily interpreted: S65°E-directed σ_1. At all three areas involving strike-slip deformation bands, the acute bisector between right- and left handed shear zones is around S60°E, in good agreement with the σ_1 orientation derived for dip-slip deformation bands at Cairn Canyon and for the stylolites at all locations. The fact that shear zone orientations show no marked improvement (or degradation) in clustering when bedding is returned to horizontal is taken as evidence that formation of the deformation bands was coeval with monoclinal folding.

3.1.3. Synthesis

Given the consistency of σ_1 directions interpreted from different types of structures at different locations along the monocline, we interpret a σ_1 direction for the San Rafael Swell of S60°E. This is in good agreement with more limited studies by Davis (1999) and Christensen and Fischer (2000) as well as the joint studies of Kelley and Clinton (1960). This is also consistent with the observed change from dominantly right-handed strike-slip motion on the southern ENE-striking section of the monocline to dominantly dip-slip deformation on the northern NNE-striking section.

On the basis of their orientation with respect to bedding, it is also possible to infer a sequence of structural formation. Stylolites appear to have formed in the very early stages of monoclinal folding while the deformation bands are inferred to be later and were probably active during much of the progressive folding of the San Rafael monocline as shown by the multiple, cross-cutting generations in Cairn Canyon.

3.2. Miners Mountain

The smallest of the uplifts in this study, Miners Mountain, is located in the northern third of Capitol Reef National Park on the western edge of the Colorado Plateau (Fig. 8). Though it is commonly portrayed on schematic maps as a part of the Circle Cliffs uplift, it is in fact a distinct structure (Anderson and Barnhard, 1986; Bump et al., 1997), albeit one that brushes the northern end of the Circle Cliffs. Like the San Rafael Swell, it is an asymmetrical, doubly-plunging anticline, the axis of which trends N60°W. In map view, the uplift is wedge shaped, tapering toward the southeast. Its northern side is a broad homocline while to the southwest it is bounded by the Teasdale monocline, which is cut by the Teasdale fault for much of its length. At its maximum, near Pleasant Creek Canyon, the fault has about 150 m of stratigraphic separation. This figure tapers rapidly toward the southeast and more gradually toward the northwest (Billingsley et al., 1987). Macroscopic deformation on Miners Mountain is limited to this fault zone, the monocline (beyond the fault tips), and to a series of small, high-angle normal faults that cut the crest of the uplift. Mapping for this study (Fig. 8) focused on the Teasdale fault and associated meso-scale structures. The lowest exposures of the fault are in the Permian Cutler Group and are characterized by a relatively wide zone of pervasive outcrop-scale faulting and occasional deformation bands. The next unit up, the Permian Kaibab Limestone, contains several horizons with small chert nodules, typically 2–5 cm in diameter, which host well-developed Eshelby joints. Higher still, the Teasdale fault is well-exposed in the basal member of the Triassic Chinle Formation, as are a series of short, antithetic faults. Toward the northwest end of the fault, the exposure level rises into the Jurassic and is marked by penetrative, conjugate Riedel deformation band arrays.

3.2.1. Deformation bands

Well-developed conjugate strike-slip deformation bands are associated with the Teasdale monocline along its entire length in the sandstones of the Jurassic Wingate and Navajo Formations and the Permian Cutler Group. Slip sense and direction are interpreted from Riedel geometries. While both right- and left-handed zones are abundant, they are generally not equally developed. The left-handed ones tend to be more numerous and wider than their right-handed counterparts. Nevertheless, the acute bisector between right- and left-handed deformation band orientations is virtually the same at all stations: N60°E (Fig. 8). Rotation of the orientation such that bedding is returned to horizontal changes this to approximately N70°E but leads to no marked improvement in the clustering of orientations.

The timing of deformation banding (relative to folding) is unclear. The fact that orientations show no change in clustering when bedding is returned to horizontal is perhaps an indication that deformation bands were actively forming throughout the period of monoclinal folding. Consequently, the σ_1 direction is interpreted as N60°E–N70°E, based on the orientation of the acute bisector between the conjugate arrays.

3.2.2. Eshelby joints

Systematic Eshelby joints were found only in close proximity to the Teasdale monocline. In all locations, the

primary joint set within Eshelby inclusions strikes about N70°E (Fig. 8). A secondary, rather poorly developed set is locally present, striking approximately perpendicular to the first. The Kaibab Limestone, which contains these inclusions, is exposed only near the upper hinge of the monocline. The beds hosting measured inclusions are everywhere within 10° of horizontal and usually much closer. Thus no attempt has been made to rotate the measured orientations.

We interpret the consistent joint orientation as the σ_1/σ_2 plane. σ_3 is thus perpendicular to that, i.e. N20°W, which is compatible with the σ_1 direction arrived at through study of deformation bands.

3.2.3. Synthesis

Inversion of both deformation bands and Eshelby joints indicates that Miners Mountain was deformed by a σ_1 oriented N60°–70°E. Given the predominance of left-handed deformation bands and the N55°W strike of the Teasdale monocline/fault within the context of this stress field, we conclude that the Teasdale monocline formed in response to left-handed oblique slip, similar to the conclusion reached by Anderson and Barnhard (1986) in their study of brittle meso-scale faults on Miners Mountain.

3.3. Monument uplift

The largest uplift in this study, the Monument extends from northeastern Arizona northward nearly halfway across Utah (Fig. 9). Though its northern and western margins are indistinct, the structural high measures approximately 210 km by 65 km (Kelley, 1955). The uplift is bounded on its southeastern margin by the Comb Ridge monocline, which extends from Blanding, Utah to Kayenta, Arizona. The northern section of the monocline, from Blanding to Bluff, Utah, trends due north and has a constant maximum dip of approximately 25°E. At Bluff, the trend of the monocline makes a sharp 30° bend to the southwest and bedding steepens to a maximum dip of 50°E. This transition is marked by an ENE-striking shear zone that cuts the monocline, extending from a point just east of the monocline westward toward Mexican Hat, Utah (Fig. 9; Hintze, 1980). This shear zone not only separates the monoclinal dip domains but also marks the northern termination of the Raplee anticline, a west-facing asymmetric anticline located immediately to the west of the Comb Ridge and occupying a position on top of and subsidiary to the Monument Uplift. South of the fault, the Comb Ridge bends westward to a trend of N60°E and maximum bedding dip shallows. The Comb Ridge terminates near Kayenta, Arizona where it is replaced by the SW-striking Cow Springs monocline and the NNE-striking Organ Rock monocline, both of which face east.

The Comb Ridge is dominated at the mesoscopic scale by penetrative jointing. Additional outcrop-scale structures have been discovered in one location: the shear zone near Bluff and Mexican Hat, Utah. The zone is continuously exposed in Pennsylvanian through Jurassic rocks and displays a wide array of penetrative structures, which relate to the variation in rock types. At its stratigraphically lowest exposure in the limestone of the Pennsylvanian Honaker Trail Formation, the shear zone is marked by conjugate faults, stylolites and well-developed en échelon vein arrays. In some places abundant red chert nodules, 10–30 cm in diameter, are also present. Along the shear zone, these host well-developed Eshelby joints. Above the Honaker Trail Formation, the sandstones of the Permian Cutler Group host conjugate faults, often with well-developed slickenlines. Continuing up-section, the Triassic Moenkopi and Chinle mudstones display only conjugate faults. At its highest level in the Jurassic Wingate, Kayenta and Navajo Sandstones, the shear zone is characterized by abundant conjugate Riedel deformation band arrays.

3.3.1. Eshelby joints

Chert inclusions within the study area contain at least one and often two systematic Eshelby joint sets. One is a through-going, planar set while the other is less planar and generally abuts the first. We interpret the first of these as the earlier and focus on that one. Joints of this set strike about S70°E and are generally perpendicular to bedding (Fig. 9), which dips from 0° to 30°. Clustering of orientations improves when they are rotated to return bedding to horizontal.

As with other joint sets in this study, we interpret the average joint orientation as the σ_1/σ_2 plane. σ_3 is thus perpendicular to that, i.e. N20°E. The consistently bed-perpendicular attitude of the joints further suggests that these joints formed relatively early in the development of the Monument uplift when bedding was still close to horizontal.

3.3.2. En échelon vein arrays

En échelon vein arrays consist here of conjugate arrays of calcite veins and stylolites. Individual veins and stylolite surfaces are typically 2–6 cm in length along strike and the entire arrays range in strike length from about 1 to 5 m. Following the methodology outlined above, en échelon vein arrays are plotted on the basis of the attitude of the array as a whole. Orientations are consistently very steep with the acute bisector between left- and right-handed arrays striking S70°E (Fig. 10). Plotted individually, both veins and stylolite teeth from within the arrays show a wide scatter in orientations though the acute bisector between those from left- versus right-handed arrays is S70°E for the veins and S60°E for the stylolite teeth. Clustering of vein array orientations improves slightly when bedding is returned to horizontal, which is significant as dip of the host bedding never exceeds 25°. Right-handed arrays tend to outnumber left-handed ones by a margin of roughly 2:1.

We interpret the acute bisector between right- and left-handed arrays, i.e. S70°E, as the σ_1 directions. We interpret the scatter in the orientations of individual

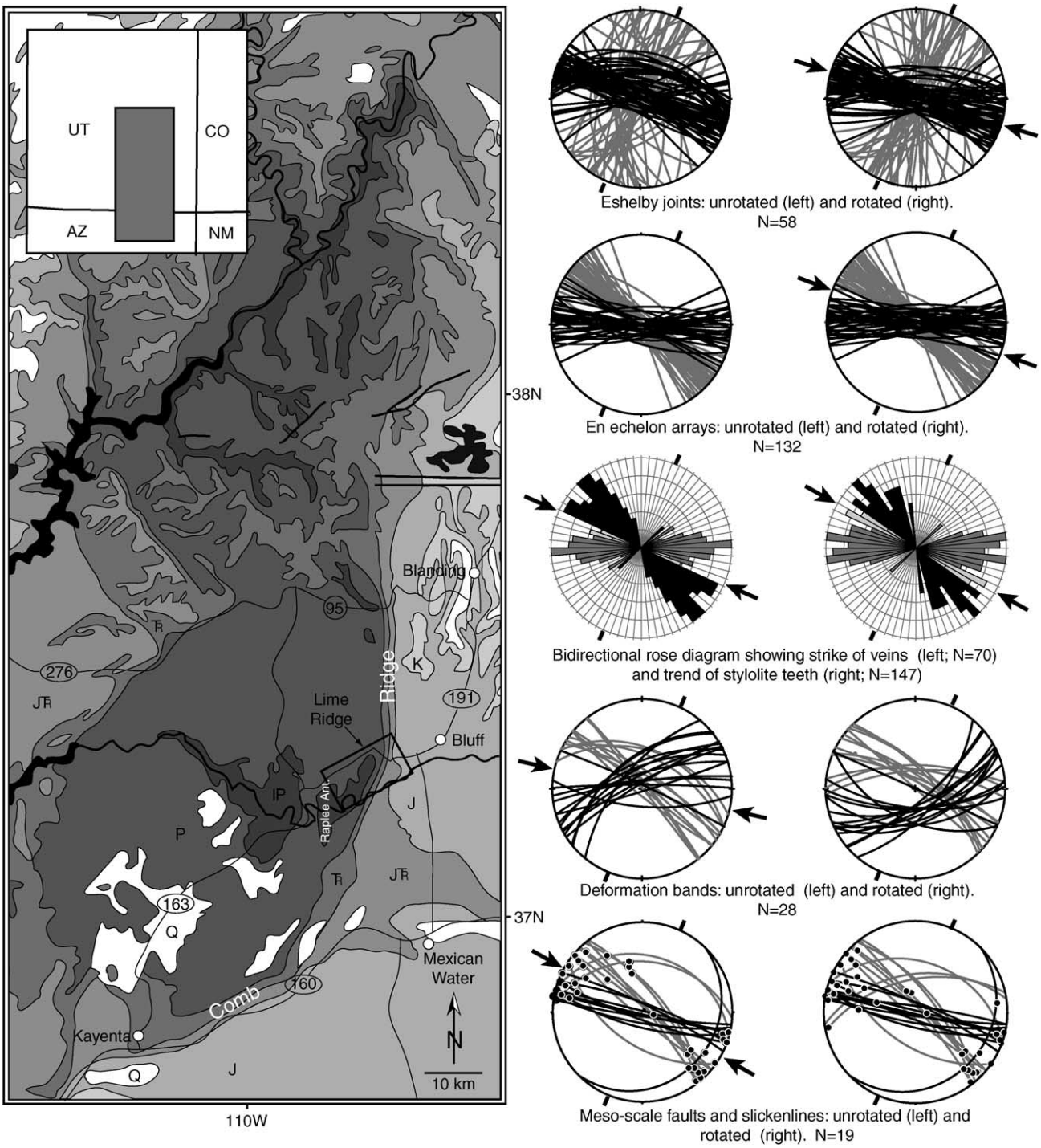

Fig. 9. Map of the Monument uplift (after Bennison, 1990) and lower hemisphere equal area stereonets for structures from the Lime Ridge area. Plot of Eshelby joints shows the primary joint set in black and the secondary one in gray. In all other plots, left-handed structures are shown in gray and right-handed structures are shown in black. The two rose diagrams are biaxial and show veins and stylolites measured within en échelon vein arrays. Those structures (stylolites and veins) measured within right-handed en échelon arrays are shown in black while those from left-handed arrays are shown in gray. Areas of overlap between left- and right-handed structures on the rose diagrams are shown in light gray. Orientations are shown both as measured ('unrotated') and rotated such that bedding is returned to horizontal ('rotated'). Paired arrows on each plot show the interpreted σ_1 direction based on the information within that plot. Paired heavy black tick marks on the outside of each plot show the local strike of the basement fault (which is assumed to parallel the strike of the monocline). Location map shows the area portrayed in Fig. 1.

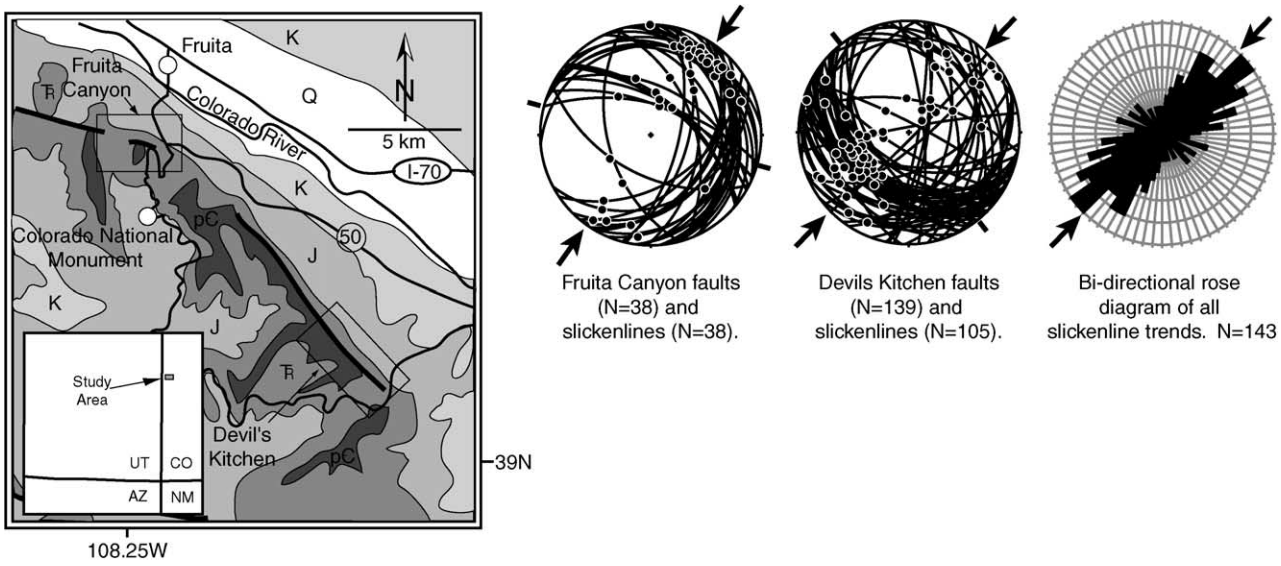

Fig. 10. Map of the northeastern Uncompahgre uplift (after Tweto, 1979) and lower hemisphere equal area stereonets showing orientations of reverse faults and slickenlines. Rotated orientations are not shown as there are multiple generations of cross-cutting faults, each of which appears to have formed, slipped, and locked up as monoclinal folding rotated them out of favorable alignment with the stress field. Restoration of bedding to horizontal thus does not yield any appreciable improvement in clustering of fault orientations. Rose diagram is biaxial and shows all slickenlines from both areas. Paired arrows on each plot show the interpreted σ_1 direction based on the information within that plot. Paired heavy black tick marks on the outside of each plot show the local strike of the basement fault (which is assumed to parallel the strike of the monocline). Location map shows the area portrayed in Fig. 1.

veins and stylolite teeth to be the result of rotation of those structures during progressive shear on their host arrays. The acute bisector may be interpreted as the σ_1 direction because the sense of rotation is opposite for left- and right-handed arrays and because both types of structures would presumably originate in the same orientation, regardless of the sense of their host array. This interpretation is in good agreement with the interpretation derived above and with the σ_3 direction interpreted from Eshelby joints. The improvement in clustering of array orientations with the restoration of bedding shows that these structures formed early relative to large-scale folding.

3.3.3. Deformation bands

Deformation bands display conjugate strike-slip orientations very similar to those recorded for the en échelon veins (Fig. 10). Left-handed bands typically strike about S50°E and right-handed ones typically strike N70°E. Although there is some scatter in the strike orientations, there is a clear separation between all right-handed bands and all left-handed ones. When rotated such that bedding is returned to horizontal, the complete separation in strike between left- and right-handed shear zones is lost as the outlying orientations from both groups begin to overlap.

We interpret this as evidence that the deformation bands formed relatively late in the construction of the Monument uplift, when bedding was already substantially folded. The unrotated deformation bands indicate a σ_1 directed S70°E.

3.3.4. Meso-scale faults

Meso-scale faults are generally very steep and exhibit predominately strike-parallel slickenlines (Fig. 9). The acute bisector between right- and left-handed faults is S60°E, similar to that for the en échelon arrays. Also like those structures, there is evidence of unequal shear: right-handed faults are typically much longer and show greater displacement than left-handed ones, although the two groups are mutually cross-cutting. Restoration of bedding to horizontal increases the scatter in fault orientations.

Based on the relationship between faults and bedding orientations, faulting seems to have been active primarily in the later stages of monocline construction. The predominance of right-handed faults implies that faulting helped to accommodate right-handed shear along the large-scale shear zone described above. Based on the orientation of the acute bisector between right- and left-handed faults, we interpret a σ_1 direction of S60°E.

3.3.5. Synthesis

Individually and collectively, all of the structures reported here point to a σ_1 trending about S70°E and a σ_3 trending N20°E, in good agreement with previous joint studies (Kelley and Clinton, 1960; Ziony, 1966). The relationships between individual structural orientations and the current orientation of the respective host beds also allow the deduction of the following sequence of structural formation: (1) Eshelby joints and en échelon vein arrays, and (2) deformation bands and brittle faults. We interpret this as a reflection of progressively increasing stress in the cover during construction of the Monument uplift.

3.4. Uncompahgre uplift

The Uncompahgre uplift is a broad, NW–SE-trending anticline extending from western Colorado into easternmost Utah (Fig. 10). The north end plunges toward the Uinta basin while the southern end is obscured beneath the San Juan volcanic field (Tweto, 1979). The uplift is about 185 km long and 40 km wide with a relatively level crest bounded on both sides by monoclinal folds, which vary in dip along strike. Unlike the other uplifts described here, basement is exposed on the Uncompahgre uplift, as is the bounding fault on the northeast side of the uplift. The maximum structural relief is approximately 1.2 km (Kelley, 1955), most of which is a product of Pennsylvanian Ancestral Rockies tectonism, which raised the Ancestral Uncompahgre uplift along a NE-dipping thrust (Stone, 1977). The Uncompahgre uplift experienced uplift again during the Laramide orogeny, this time along two faults, one on the southwest side and a new one on the northeast side (Stone, 1977). The fault on the northeast side of the uplift is exposed in canyons of the Colorado National Monument, near Grand Junction on the northeast side of the uplift where the fault curves from a strike of S40°E in the Devils Kitchen area (see Fig. 10) to S75°E in the Fruita Canyon area. Although this fault is locally very well exposed, it is devoid of structures that might reveal the slip direction. The ridges between those canyons, however, preserve monoclinally folded cover sediments that have been highly attenuated during folding. In particular, the Jurassic Wingate Sandstone has been stretched across the middle limb of the monocline and in the process, thinned by up to 40% (Jamison and Stearns, 1982). Thinning is accomplished by slip on penetrative deformation bands, many of which exhibit slickenlines. The magnitude of slip is generally only a few centimeters. Because of the attractive exposures within the Monument and the relatively heavy vegetation and low strain elsewhere, fieldwork was concentrated on the exposures described above. Data are limited to deformation bands alone.

3.4.1. Deformation bands

At both the Devils Kitchen and Fruita Canyon areas, deformation bands display a wide array of orientations (Fig. 11). Slickenlines at both areas, however display a consistent NE–SW trend. At Devils Kitchen, the median slickenline trend is approximately N55°E, which is perpendicular to the local strike of the uplift-bounding fault. At Fruita Canyon, the median slickenline trend is approximately N35°E, which is oblique to the local strike of the uplift-bounding fault (S75°E). To be exact, it is 20° east of perpendicular to the strike of that fault, placing it somewhere between pure dip-slip and parallelism with the Devils Kitchen median.

If these deformation bands reflected only passive thinning of the middle limb of the monocline and revealed nothing of the shortening direction of the Uncompahgre uplift as a whole, one might expect that they would everywhere show dip-slip, regardless of the strike of the uplift-bounding fault. On the other hand, if the sedimentary cover were firmly welded to the basement such that stretching of the middle limb must be everywhere parallel to the slip vector for the Uncompahgre uplift as a whole, then one might expect slickenlines to be parallel everywhere, regardless of the strike of the uplift-bounding fault. In this case, reality appears to lie somewhere between these two end-member scenarios. It seems reasonable that the σ_1 direction for the Uncompahgre uplift is generally NE and perhaps N50°–55°E, since the Devils Kitchen deformation bands show no systematic oblique slip. This is in general agreement with previous work (Jamison and Stearns, 1982).

4. Discussion

4.1. Relationship of cover stress to basement strain

Fig. 11 integrates the interpretations of this study into a detailed picture of the principal stress axes associated with each uplift. As Kelley and Clinton (1960) proposed, there are two families of orientations. The sedimentary cover over both the San Rafael Swell and the Monument uplift exhibits WNW–ESE-directed stress. Cover on Miners Mountain and the Uncompahgre uplift shows NE–SW-directed stress. Incorporating the results of other detailed studies, the Kaibab uplift (Tindall and Davis, 1999) and Circle Cliffs uplift (Anderson and Barnhard, 1986; Roznovsky, 1998; Davis, 1999) both reveal NE–SW-directed stress in the cover. Collectively, these interpretations raise a number of questions. How far may these stress orientations be extrapolated? How do they relate to deformation of the basement? What does this reveal about the regional kinematics?

Both the regional strain patterns and the available timing data indicate that the stress states interpreted here are only locally valid. Although many of the stratigraphic units examined in this study are exposed in areas remote from any monocline (Fig. 1), they show the type of penetrative deformation described here only in exposures within the monoclines. This indicates to us that only in the immediate vicinity of the monoclines were stresses high enough to generate penetrative deformation, which in turn suggests that the stress states interpreted here are valid only for their respective host monoclines. This is further supported by interpretations of uplift timing (and by inference the timing of the small-scale structures described here). Sedimentologic work near the Kaibab uplift (Goldstrand, 1994) and San Rafael Swell (Lawton, 1983b) indicates that both of those uplifts rose at about the same time. Assuming that this is true, the differently-oriented stress states interpreted for those two uplifts must necessarily be local phenomena.

The observation of localized high strain zones and the interpretation of variously-oriented local stress states further implies that the regional stresses (i.e. those that actually

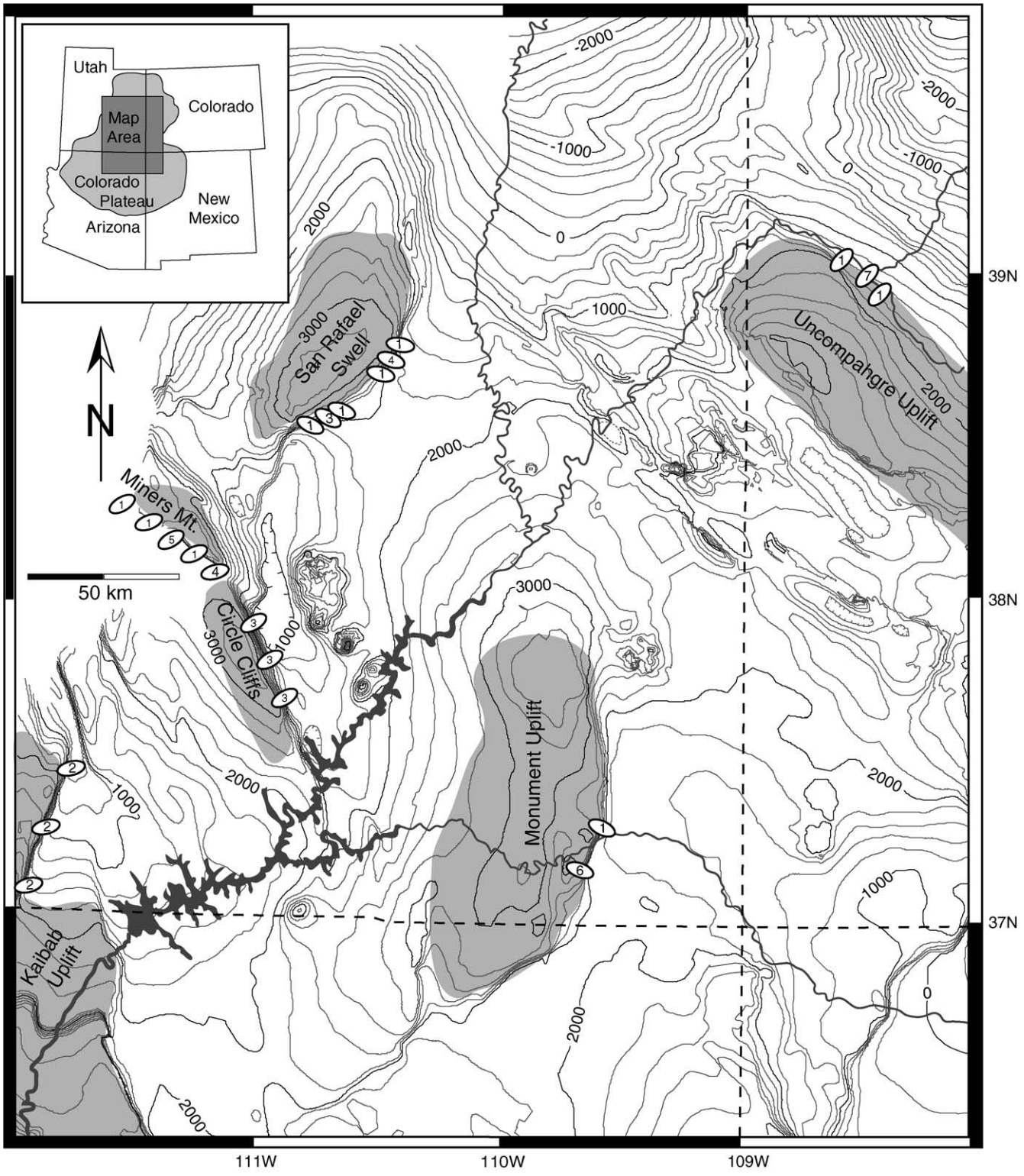

Fig. 11. Structure contour map of the northern Colorado Plateau showing the approximate areas of the uplifts (shaded gray) in this study. Contours are drawn at 200 m intervals on the base of the Cretaceous Dakota Sandstone (modified after Baker, 1935; O'Sullivan, 1963; Williams, 1964; Williams and Hackman, 1971; Haynes et al., 1972; Cashion, 1973; Hackman and Wyant, 1973; Haynes and Hackman, 1978). Structural elevations are in meters above sea level. Ellipses show local paleostress directions (though not magnitudes). Numbers inside ellipses refer to source of interpretation: 1. this study; 2. Tindall and Davis (1999); 3. Davis (1999), Anderson and Barnhard (1986), and Roznovsky (1998); 4. Davis (1999); 5. Anderson and Barnhard (1986); 6. Ziony (1966); 7. Jamison and Stearns (1982). The Colorado River and its tributaries are shown for reference in dark gray.

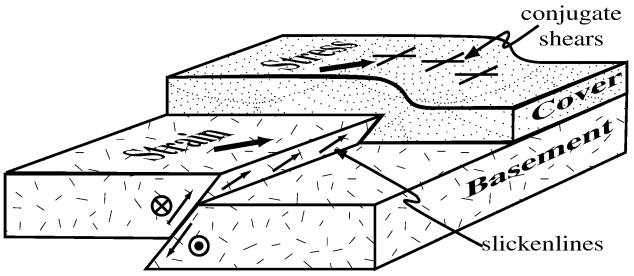

Fig. 12. Schematic block diagram showing the relationship between basement strain and cover stress. Slip on the basement fault in this example is oblique right-handed reverse. Penetrative deformation in the cover (shown here as conjugate shears) is localized along the monocline above the basement fault and reveals principal stress directions parallel to the principal strain directions in the basement.

drove monoclinal folding) were transmitted not through the cover but at a deeper crustal level, perhaps in the crystalline basement (Erslev, 1993; Davis, 1999). Only in those places where the strong basement beam failed were stresses transferred to the cover, creating the deformation observed at the surface. Assuming that cover was welded to basement, such that they could not move independently, cover *stress* was created by basement *strain*. In other words, the direction of greatest shortening in the basement was parallel to the maximum compressive stress direction in the cover (Fig. 12). That cover was in fact welded to the basement is indicated by observations of oblique slip along some monoclines, which indicates that basement could not move laterally without moving the cover with it (Anderson and Barnhard, 1986; Davis, 1999; Tindall and Davis, 1999). Further assuming that the cover was isotropic, the interpreted cover *stress* directions can be viewed as basement *strain* directions. Basement strain, in turn was presumably controlled by the regional stresses set up by plate interactions.

This concept is perhaps best illustrated by the clay cake experiments of Cloos (1928) and Riedel (1929). The experimental set-up consisted of two parallel boards (analogous to basement) overlain by a wet clay cake (analogous to sedimentary cover). Subjected to a horizontal stress, the system failed along the interface between the two boards, allowing slip between them and creating a series of en échelon faults (Riedel shears) in the clay immediately above the interface. Deformation in the clay cake was restricted to that zone because elsewhere (away from the 'basement fault') the regional stresses were supported by the strong boards. Similarly, the stress directions reflected by deformation in the clay were controlled by the relative movement of the boards and did not necessarily reflect regional stress conditions (Cloos, 1928; Riedel, 1929).

The key assumption in this argument is that the cover is effectively welded to the basement. While this is easily verified in clay cake experiments where one can watch the 'basement-cover' interface during deformation, it is less straightforward with regard to the Colorado Plateau. The geology exposed at the surface today is underlain in most places by multiple potential detachment horizons, including the Cambrian Bright Angel Shale, the interbedded salts and shales of the Pennsylvanian Paradox Formation, and the shales of the Triassic Chinle Formation (Hintze, 1988). Two arguments suggest that these did not in fact decouple the cover and basement during the Laramide. First, the ratio of cover area to detachment horizon thickness is enormous. The shales of the Chinle and Bright Angel Formations are at most about 200 m thick and the Paradox Formation reaches a maximum thickness of about 3000 m beneath Canyonlands National Park and the northern Monument uplift (Hintze, 1988). These are not insignificant thicknesses but they pale in comparison with the surface areas of the uplifts which range from $\sim$800 km^2 for Miners Mountain to $\sim$4000 km^2 for the Monument uplift (Hintze, 1980). The force transmitted from basement to the currently exposed levels of the cover is the product of shear stress times area. In order to decouple the cover from the basement, the shear strength of the detachment horizons would have to have been near zero. Although weak, shales do have some shear strength (Jaeger and Cook, 1976). That, combined with their relatively small thicknesses, leads us to believe that the shales were not significant detachment horizons. The Chinle Formation is also exposed in most of the monoclines described here and we have observed no evidence of significant shear within it. Salt horizons within the Paradox Formation are more problematic as they are both thicker (Hintze, 1988) and weaker (Jaeger and Cook, 1976) than the shales described above. The possibility has to be allowed that in the Four Corners area where they reach their maximum thickness, they may decouple the currently exposed level of the cover from basement.

The second argument comes from this study and is the observation that measured stress directions are consistently oriented within each uplift, independent of the strike of the bounding monocline. The cover on top of each uplift everywhere moves in the same direction relative to a reference point in the neighboring basin. If the cover were detached from the basement, it is expected that all deformation would be the subsidiary result of vertical displacements and monoclinal folding.

4.2. Basement kinematics and fault geometry

Acting on the idea that cover stress directions reflect basement strain directions, the ellipses presented in Fig. 11 may be viewed not only as depictions of the local stress state in the cover but also as depictions of the local basement strain directions. Inspection of the structural contours in Fig. 11 also suggests patterns of the basement strain magnitude. A minimalist view would be to assume that the basement faults responsible for monoclinal folding in the cover have a strike-length equal to that of the overlying monocline. It is recognized that some or even all of these faults may in fact be much longer than that, as interpreted in various studies of tectonic lineaments (e.g. Kelley and Clinton, 1960; Davis,

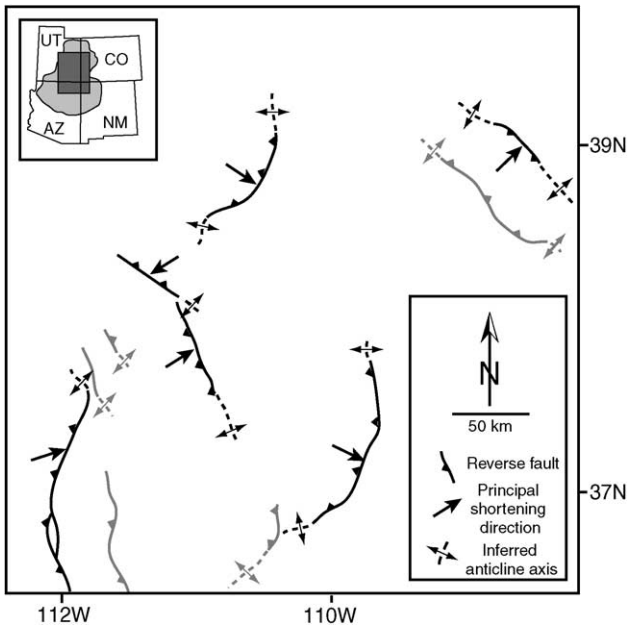

Fig. 13. Interpreted map of Late Cretaceous–early Tertiary basement deformation on the northern Colorado Plateau. Basement faults are interpreted beneath each of the major monoclines. Black faults are ones for which kinematics may be reasonably interpreted, based on this and previous studies. Arrows show heave directions for those faults. Gray faults underlie smaller monoclines which have not been extensively studied. It should be noted that this is a minimalist interpretation that includes only those faults that were clearly active during the Laramide orogeny. In no way does this interpretation preclude the existence of other faults or lineaments.

1978; Maughan and Perry, 1986). However, if the faults do extend significantly farther, the sections beyond the tips of the monoclines could not have slipped much as shown by the lack of corresponding deformation in the cover. This raises the issue of how the assumed faults tip out. The question is whether their ends are defined by tears that decouple them from the neighboring rock or whether slip is transferred along strike to some other structure(s). No evidence of significant tears in the cover near the ends of these monoclines has ever been reported and it seems unlikely that the same basement that appears welded to cover along the monoclines could be completely detached from the cover elsewhere such that basement tears would produce no appreciable deformation in the cover. The possibility of major tear faults is therefore discounted. Alternatively, fault strain may be transferred along strike to broad basement arches. This idea is supported by much of the secondary map pattern (i.e. beyond the major uplifts) of the Colorado Plateau. For example, the Henry basin (approximately defined by the limits of the Cretaceous strata immediately east of the Circle Cliffs uplift in Fig. 1) is bounded both by uplifts described in this study and by broad, linear structural highs (defined by Jurassic rocks in Fig. 1; see also Fig. 11) that continue approximately along strike from the ends of the uplifts. From the southern end of the San Rafael Swell, a swath of Jurassic rock (bounded on both sides by Cretaceous) continues southwestward to Miners Mountain. From the southern end of the Circle Cliffs uplift, a similar belt of Jurassic rock continues along strike to the Monument uplift. The Monument uplift and a third band of Jurassic rock that connects its northern tip to the San Rafael Swell complete the circle that defines the Henry basin. A similar arch extends SW from the end of the Monument uplift (Figs. 1 and 11). On the basis of this evidence, it seems reasonable to say that slip on the presumed basement faults in the cores of these monoclines is transferred along strike into broad arches. This also implies that the basement faults (or at least the sections of them that were active in the Laramide orogeny) do not interconnect, and thus do not divide the foreland basement into a series of discrete, jostling blocks. We propose that a more accurate view is that of a set of unconnected cuts within a continuous sheet of basement, similar to tears in a blanket (Fig. 13).

4.3. Regional implications

The inferred kinematics of the interpreted basement faults show that the assumption of dip-slip, used by Kelley and Clinton (1960), and currently assumed at a 90% confidence level by Bird (1998) in his Laramide reconstruction of the Colorado Plateau, need not apply. It is simply not supportable to assume that each uplift and associated monocline is the result of a dip-slip displacement as there is clear evidence of oblique slip along some of them. Both the Kaibab uplift (Tindall and Davis, 1999) and Miners Mountain (Anderson and Barnhard, 1986; this study) formed under oblique slip all along their length. To a lesser degree, the curved traces of the San Rafael Swell (Davis, 1999; this study) and the Monument uplift (this study) both exhibit oblique slip along parts of their length. (e.g. Anderson and Barnhard, 1986; Bump et al., 1997; Tindall and Davis, 1999).

Furthermore, the kinematic interpretations of this study do not support the model proposed by Yin (1994) in which the monoclines developed by flexural slip in response to regional arching of the Plateau. Yin's (1994, fig. 7) computed σ_1 trajectories[1] in the northwestern Plateau are consistently NE- to NNE-trending, implying that the uplifts covered by the present study should all be characterized by similarly directed oblique slip. For the Uncompahgre uplift, this prediction approximately matches the shortening direction interpreted here. For the remaining five uplifts discussed here, however, Yin's (1994) computed stress direction disagrees with the results of the present study by 30–90°.

[1] In the notation of this paper, these are 'regional' or 'basement' σ_1 trajectories and are not equivalent to the 'cover stresses' described in this paper. Rather, they drive basement deformation, which in turn would set up stress in the cover.

5. Conclusions

In addition to joints, the Laramide uplifts of the Colorado Plateau are hosts to a number of small-scale structures including Eshelby joints, deformation bands, stylolites, en échelon arrays of semi-brittle structures, and meso-scale faults. These structures interpreted in combination can yield reliable paleostress directions for the sedimentary cover of the monoclines on which they are developed. Mapping and analysis of these structures reveals principal compression directions in the cover of S60°E and S70°E for the San Rafael Swell and Monument uplift, respectively, and N60°E and N50°E for Miners Mountain and the Uncompahgre, respectively. Cover stress directions (interpreted from cover strain indicators) may be viewed as basement strain directions if the cover is approximately welded to basement, which we believe is the case for the northern Colorado Plateau. Our work lends support and further precision to the kinematic interpretations of Kelley and Clinton (1960) and highlights the importance of oblique slip in creating the uplifts described here. Finally, examination of structural contours allows interpretation of basement strain magnitudes and suggests that the major faults active in the Laramide orogeny are not long, interconnected features but are tears that are wholly contained within a continuous basement.

Acknowledgements

This work was supported by a GSA Penrose Grant, the L. Austin Weeks AAPG Grant-in-Aid and by grants from the Geostructure Partnership and the Department of Geosciences at the University of Arizona. Thanks to Steve Ahlgren, Scott Miller, Steve Kidder, Greg Bilinski and Amos Sanders for their assistance in the field. This manuscript has benefited from reviews by Steve Ahlgren, Steve Cather, Clem Chase, John Craddock, and Chuck Kluth and Jim Evans. Our thanks to all of them.

References

Allmendinger, R., Hauge, T., Hauser, E., Potter, C., Klemperer, S., Nelson, K., Kneupfer, P., Oliver, J., 1987. Overview of the COCORP 40 degree N Transect, western United States: the fabric of an orogenic belt. Geological Society of America Bulletin 98, 308–319.

Anderson, R.E., Barnhard, T.P., 1986. Genetic relationship between faults and folds and determination of Laramide and neotectonic paleostress, western Colorado Plateau transition zone. Tectonics 5, 335–357.

Aydin, A., 1978. Small faults formed as deformation bands in sandstone. Pure and Applied Geophysics 116, 913–930.

Aydin, A., Johnson, A.M., 1983. Analysis of faulting in porous sandstones. Journal of Structural Geology 5, 19–31.

Baker, A.A., 1935. Geologic structure of southeastern Utah. Bulletin of the American Association of Petroleum Geologists 19, 1472–1507.

Bennison, A.P., 1990. Geological Highway Map of the Southern Rocky Mountain Region. American Association of Petroleum Geologists, Tulsa, OK.

Bergerat, F., Bouroz-Weil, C., Angelier, J., 1992. Paleostresses inferred from macrofractures, Colorado Plateau, western USA. Tectonophysics 206, 219–243.

Billingsley, G.H., Huntoon, P.W., Breed, W.J., 1987. Geologic Map of Capitol Reef National Park and Vicinity, Emery, Garfield, Millard and Wayne Counties, Utah. Utah Geological and Mineral Survey, Salt Lake City.

Bird, P., 1998. Kinematic history of the Laramide orogeny in latitudes 35–49N, western United States. Tectonics 17, 780–801.

Brown, W.G., 1988. Deformation style of Laramide uplifts in the Wyoming foreland. In: Schmidt, C.J., Perry, W.L.J. (Eds.), Interaction of the Rocky Mountain Foreland and the Cordilleran Thrust Belt. Geological Society of America Memoir 171, pp. 1–25.

Brown, W.G., 1993. Structural style of Laramide basement-cored uplifts and associated folds. In: Snoke, A.W., Steidtmann, J.R., Roberts, S.M. (Eds.), Geology of Wyoming. Geological Survey of Wyoming Memoir No. 5, pp. 312–371.

Bump, A.P., Ahglren, S.G., Davis, G.H., 1997. A tale of two uplifts: Waterpocket Fold, Capitol Reef National Park. Eos (Tansactions, American Geophysical Union) 78, F701.

Cashion, W.B., 1973. Geologic and Structure Map of the Grand Junction Quadrangle, Colorado and Utah. United States Geological Survey, Washington.

Christensen, R.D., Fischer, M.P., 2000. Using mesoscopic structural analysis to interpret the deformation history of the San Rafael Swell, east-central Utah. Geological Society of America 2000 Annual Meeting Abstracts with Program, 32 pp.

Cloos, H., 1928. Experimenten zur inneren Tektonik. Zentralblatt fur Mineralogie und Paleontologie 1928B, 609.

Cook, K.L., Mabey, D.R., Bankey, V., 1991. The new gravity map of Utah—an overview of its usefulness for geologic studies. Utah Geologic and Mineral Survey Notes 24, 12–21.

Craddock, J.P., van der Pluijm, B.A., 1988. Kinematic analysis of an en échelon-continuous vein complex. Journal of Structural Geology 10, 445–452.

Davis, G.H., 1978. Monocline fold pattern of the Colorado Plateau. In: Matthews, V.I. (Ed.), Laramide Folding Associated with Basement Block Faulting in the Western United States. Geological Society of America Memoir 151, pp. 215–233.

Davis, G.H., 1999. Structural Geology of the Colorado Plateau Region of Southern Utah with Special Emphasis on Deformation Bands. Geological Society of America Special Paper 342.

Davis, G.H., Reynolds, S.J., 1996. Structural Geology of Rocks and Regions. John Wiley & Sons, New York.

Davis, G.H., Bump, A.P., Garcia, P.E., Ahlgren, S.G., 2000. Conjugate Riedel deformation band shear zones. Journal of Structural Geology 22, 169–190.

Dickinson, W.R., Klute, M.A., Hayes, M.J., Janecke, S.U., Lundin, E.R., McKitterick, M.A., Olivares, M.D., 1988. Paleogeographic and paleotectonic setting of Laramide sedimentary basins in the central Rocky Mountain region. Geological Society of America Bulletin 100, 1023–1039.

Dumitru, T., Duddy, I., Green, P., 1994. Mesozoic–Cenozoic burial, uplift, and erosion of the west-central Colorado Plateau. Geology 22, 499–502.

Dunne, W.M., Hancock, P.L., 1994. Paleostress analysis of small-scale brittle structures. In: Hancock, P.L. (Ed.). Continental Deformation. Pergamon Press, New York, pp. 101–120.

Dutton, C.E., 1882. The physical geology of the Grand Canyon district. United States Geological Survey Second Annual Report, pp. 49–166.

Eardley, A.J., 1949. Structural evolution of Utah. In: Hansen, G.H., Bell, M.M. (Eds.). The Oil and Gas Possibilities of Utah. Utah Geological and Mineral Survey, Salt Lake City, pp. 10–23.

Eidelman, A., Reches, Z., 1992. Fractured pebbles—a new stress indicator. Geology 20, 307–310.

Erslev, E.A., 1993. Thrusts, back-thrusts, and detachment of Rocky Mountain foreland arches. In: Schmidt, C.J., Chase, R.B., Erslev, E.A. (Eds.),

Laramide Basement Deformation in the Rocky Mountain Foreland of the Western United States. Geological Society of America Special Paper 280, pp. 339–359.

Erslev, E.A., 2001. Multistage, multidirectional Tertiary shortening and compression in north-central New Mexico. Geological Society of America Bulletin 113, 63–74.

Eshelby, J.D., 1957. The determination of the elastic field of an ellipsoidal inclusion, and related problems. Proceedings of the Royal Society of London Serial A 241, 376–396.

Eyal, Y., Reches, Z., 1983. Tectonic analysis of the Dead Sea rift region since the Late Cretaceous based on mesostructures. Tectonics 2, 167–185.

Gilbert, G.K., 1876. The Colorado Plateau Province as a field for geological study. American Journal of Science 12, 16–24 see also 85–103.

Gilluly, J., 1929. Geology and oil and gas prospects of part of the San Rafael Swell, Utah. United States Geological Survey Bulletin 806, 69–130.

Goldstrand, P.M., 1994. Tectonic development of Upper Cretaceous to Eocene strata of southwestern Utah. Geological Society of America Bulletin 106, 145–154.

Gray, M.B., Mitra, G., 1993. Migration of deformation fronts during progressive deformation: evidence from detailed structural studies in the Pennsylvania Anthracite region, USA. Journal of Structural Geology 15, 435–449.

Hackman, R.J., Wyant, D.G., 1973. Geology, Structure, and Uranium Deposits of the Escalante Quadrangle, Utah and Arizona. United States Geological Survey, Washington.

Hancock, P.L., 1972. The analysis of en échelon veins. Geological Magazine 109, 269–276.

Hancock, P.L., 1985. Brittle microtectonics: principles and practice. Journal of Structural Geology 7, 437–457.

Haynes, D.D., Hackman, R.J., 1978. Geology, Structure, and Uranium Deposits of the Marble Canyon 1×2 Quadrangle, Arizona. United States Geological Survey, Washington.

Haynes, D.D., Vogel, J.D., Wyant, D.G., 1972. Geology, Structure, and Uranium Deposits of the Cortez Quadrangle, Utah and Colorado. United States Geological Survey, Washington.

Hintze, L.F., 1980. Geologic Map of Utah. Utah Geological and Mineral Survey, Salt Lake City.

Hintze, L.F., 1988. Geologic History of Utah. Brigham Young University Dept. of Geology, Salt Lake City.

Huntoon, P.W., 1993. Influence of inherited Precambrian basement structure on the localization and form of Laramide monoclines, Grand Canyon, Arizona. In: Schmidt, C.J., Chase, R.B., Erslev, E.A. (Eds.), Laramide Basement Deformation in the Rocky Mountain Foreland of the Western United States. Geological Society of America Special Paper 280, pp. 243–256.

Huntoon, P.W., Sears, J.W., 1975. Bright Angel and Eminence faults, eastern Grand Canyon, Arizona. Geological Society of America Bulletin 86, 465–472.

Jackson, M.D., Pollard, D.D., 1990. Flexure and faulting of sedimentary host rocks during growth of igneous domes, Henry Mountains, Utah. Journal of Structural Geology 12, 185–206.

Jaeger, J.C., Cook, N.G.W., 1976. Fundamentals of Rock Mechanics. Halted Press, New York.

Jamison, W.R., Stearns, D.W., 1982. Tectonic deformation of Wingate Sandstone, Colorado National Monument. AAPG Bulletin 66, 2584–2608.

Kelley, V., 1955. Regional tectonics of the Colorado Plateau and relationship to the origin and distribution of Uranium. University of New Mexico Publications in Geology 5.

Kelley, V.C., Clinton, N.J., 1960. Fracture systems and tectonic elements of the Colorado Plateau. University of New Mexico Publications in Geology 6.

Lawton, T.F., 1983. Fluvial systems of the Upper Cretaceous Mesaverde Group and Paleocene North Horn Formation, central Utah; a record of transition from thin-skinned to thick-skinned deformation in the foreland regions. In: Peterson, J. (Ed.), Paleotectonics and Sedimentation in the Rocky Mountain Region, United States. American Association of Petroleum Geologists Memoir 41, pp. 423–442.

Lawton, T.F., 1983b. Late Cretaceous fluvial systems and the age of foreland uplifts in central Utah. In: Lowell, J.D., Gries, R.R. (Eds.). Rocky Mountain Foreland Basins and Uplifts. Rocky Mountain Association of Geologists, Denver, pp. 181–199.

Lohman, S.W., 1965. Geology and Artesian Water Supply, Grand Junction Area, Colorado. U.S. Government Printing Office, Washington.

Lowell, J.D., 1983. Rocky Mountain Foreland Basins and Uplifts. Rocky Mountain Association of Geologists, Denver.

Maughan, E.K., Perry, W.J.J., 1986. Lineaments and their tectonic implications in the Rocky Mountains and adjacent Great Plains region. In: Peterson, J.A. (Ed.), Paleotectonics and Sedimentation. American Association of Petroleum Geologists Memoir 41, pp. 41–53.

Molzer, P.C., Erslev, E.A., 1992. Oblique thrusting in Laramide foreland arches. American Association of Petroleum Geologists Bulletin 76, 1265.

Nickelsen, R.P., 1972. Attributes of rock cleavage in some mudstones and limestones of the Valley and Ridge province, Pennsylvania. Pennsylvania Academy of Science Proceedings 46, 107–112.

Nickelsen, R.P., 1979. Sequence of structural stages of the Alleghany Orogeny at the Bear Valley strip mine, Shamokin, Pennsylvania. American Journal of Science 279, 225–271.

O'Sullivan, R.B., 1963. Geology, Structure, and Uranium Deposits of the Shiprock Quadrangle, New Mexico and Arizona. United States Geological Survey, Washington.

Powell, J.W., 1873. Some remarks on the geological structure of a district of country lying to the north of the Grand Canyon of the Colorado. American Journal of Science 5, 456–465.

Ramsay, J.G., Huber, M.I., 1987. The Techniques of Modern Structural Geology, Volume 2: Folds and Fractures. Academic Press, New York.

Riedel, W., 1929. Zur mechanik geologischer brucherscheinungen. Zentralblatt für Mineralogie und Paleontologie 1929B, 354.

Roznovsky, T.A., 1998. Variation in joint and fault patterns along the East Kaibab and Waterpocket Monoclines, Colorado Plateau. Unpublished Masters thesis, Stanford University.

Schmidt, C.J., Chase, R.B., Erslev, E.A., 1993. Laramide Basement Deformation in the Rocky Mountain Foreland of the Western United States. Geological Society of America, Boulder.

Shainin, V.E., 1950. Conjugate sets of en échelon tension fractures in the athens limestone at Riverton, Virginia. Geological Society of America Bulletin 61, 509–517.

Stern, S.M., 1992. Geometry of basement faults underlying the northern extent of the East Kaibab Monocline, Utah. Unpublished M.S. thesis, University of North Carolina at Chapel Hill.

Stone, D.S., 1977. Tectonic history of the Uncompahgre Uplift. In: Veal, H.K. (Ed.), Exploration Frontiers of the Central and Southern Rockies. Rocky Mountain Association of Geologists 1977 Symposium, pp. 23–30.

Strahler, A.N., 1948. Geomorphology and structure of the West Kaibab fault zone and Kaibab plateau, Arizona. Geological Society of America Bulletin 59, 513–540.

Tchalenko, J., 1970. Similarities between shear zones of different magnitudes. Geological Society of America Bulletin 81, 1625–1639.

Tindall, S.E., Davis, G.H., 1999. Monocline development by oblique-slip fault propagation folding: the East Kaibab monocline, Colorado Plateau, Utah. Journal of Structural Geology 21, 1303–1320.

Tweto, O., 1979. Geologic Map of Colorado. United States Geological Survey.

Twiss, R.J., Moores, E.M., 1992. Structural Geology. W.H. Freeman and Company, New York.

Varga, R.J., 1993. Rocky Mountain foreland uplifts: Products of a rotating stress field or strain partitioning. Geology 21, 1115–1118.

Wilcox, R., Harding, T., Seely, D., 1973. Basic wrench tectonics. American Association of Petroleum Geologists Bulletin 57, 74–96.

Williams, P.L., 1964. Geology, Structure, and Uranium Deposits of the Moab Quadrangle, Colorado and Utah. United States Geological Survey, Washington.

Williams, P.L., Hackman, R.J., 1971. Geology, structure and uranium deposits of the Salina quadrangle, Utah. United States Geological Survey, Washington.

Yin, A., 1994. Mechanics of monoclinal systems in the Colorado Plateau during the Laramide orogeny. Journal of Geophysical Research 99, 22,043–22,058.

Ziony, J.I., 1966. Analysis of systematic jointing in part of the Monument Upwarp, southeastern Utah. Unpublished Ph.D. thesis, University of California, Los Angeles.